Magnetothermopower study of the quasi-two-dimensional organic conductor α-(BEDT-TTF)$_2$KHg(SCN)$_4$

E. S. Choi
Department of Physics, Ewha Womans University, Seoul 120-750, Korea and National High Magnetic Field Laboratory, Florida State University, Tallahassee, Florida 32310

J. S. Brooks and J. S. Qualls*
National High Magnetic Field Laboratory and Physics Department, Florida State University, Tallahassee, Florida 32310
(Received 22 April 2001; revised manuscript received 22 February 2002; published 17 May 2002)

We have used a low-frequency magneto-thermopower (MTEP) method to probe the high-magnetic-field ground-state behavior of α-(BEDT-TTF)$_2$KHg(SCN)$_4$ along all three principal crystallographic axes at low temperatures. The thermopower tensor coefficients (S_{xx}, S_{yx}, and S_{zz}) have been measured to 30 T, beyond the anomalous low-temperature, field-induced transition at 22.5 T. We find a significant anisotropy in the MTEP signal, and also observe large quantum oscillations associated with Landau quantization. The anisotropy indicates that the ground-state properties are clearly driven by mechanisms that occur along specific directions for the in-plane electronic structure. Both transverse and longitudinal magnetothermopower show asymptotic behaviors in the field, which can be explained in terms of magnetic breakdown of compensated closed orbits.

DOI: 10.1103/PhysRevB.65.205119 PACS number(s): 74.25.Fy, 72.15.Jf, 75.30.Kz

I. INTRODUCTION

The ground state of the quasi-two-dimensional organic conductor α-(BEDT-TTF)$_2$KHg(SCN)$_4$ has emerged as an important problem in the area of the physics of synthetic metals in high magnetic fields. This is due to the highly unusual magnetic-field-dependent behavior of the low-temperature ground state which appears below a transition temperature $T_p = 8$ K. Band-structure calculations[1] indicate a two-dimensional Fermi surface, consisting of a quasi-one-dimensional electron section and a closed hole pocket, as shown in Fig. 1(a). Density wave formation is believed to occur below T_p due to an instability in the open Fermi surface sheets at low temperatures, which results in a Fermi-surface reconstruction with the periodicity of the density wave nesting vector.[2] This in turn leads to the unusual behavior of this compound at low temperatures and high magnetic fields.[3,4] The assignment of the ground state as a spin-density wave or a charge density wave (CDW) remains controversial.[5] Above 22.5 T, an anomaly (called the ''kink field'' or B_k after its discovery by Osada *et al.*[6]) appears in the magnetoresistance, and a high-field electronic state emerges. Studies in tilted magnetic fields[7,8] in the vicinity of B_k have indicated CDW behavior. This is, however, based on a comparison with theoretical work for a one-dimensional metal, where both spin and orbital mechanisms compete.[9] Recently the observation of critical state behavior in the magnetization[10] and susceptibility[11] above B_k has been reported, which indicates an unusual, highly conductive state which is associated with the Landau-level filling fraction. Additional thermodynamic evidence of an unusual, hysteretic behavior above B_k, which is related to the Landau-level filling, has also been reported in high-field magnetocaloric measurements.[12]

The purpose of the present work is to probe this ground state by thermoelectric power (TEP), which involves measuring the potential difference across a sample in the presence of a thermal gradient, as shown in Fig. 1(c). In general, the TEP (or more simply, the thermopower S) can be expressed by the Mott formula[13]

$$S = \frac{\pi^2 k_B^2 T}{3e} \frac{d \ln\sigma(\epsilon)}{d\epsilon}\bigg|_{\epsilon=\epsilon_F}, \tag{1}$$

where $\sigma(\epsilon)$ is the energy-dependent electrical conductivity. In addition to S, we have also measured the Nernst effect for specific sample configurations. This involves the transverse thermopower which is given in the simple approximation by $S_{xy} = QB(l/d)$, where Q is the Nernst coefficient, B is the magnetic field, and l/d is the ratio of the distance between the Nernst leads and the sample thickness. We note that, ideally, for closed orbits, S_{xy} is not sensitive to electron/hole compensation effects, and that it increases linearly with magnetic field. (See discussion below.)

Clearly the thermopower and Nernst signals can be a complex mixture of phenomena which can be difficult to interpret, unless specific aspects of the system under consideration dominate and/or change dramatically.[14] Examples include the case of a conventional metal ($S \approx k_B^2 T/e\epsilon_F$), a superconductor ($S = 0$), and the quantum Hall effect ($S \approx 0$ or a finite value depending on the Landau-level filling). As we will show in the present case, the thermopower for α-(BEDT-TTF)$_2$KHg(SCN)$_4$ is particularly sensitive to the Landau-level spectrum, to the gap in the electronic structure, and to the in-plane electronic anisotropy.

In light of the discussion above, here we state the main findings of the present work before the full presentation. *First*, where comparisons can be made with previous studies (most of which were done at low or zero magnetic fields), we find that our results agree in the details of the sensitivity of the thermopower to the anisotropic Fermi surface topology, and with the absolute values of the thermopower signals pre-

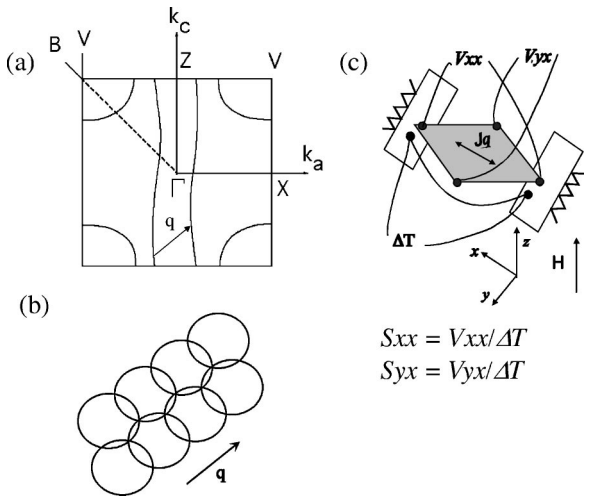

FIG. 1. Fermi surface of α-(BEDT-TTF)$_2$KHg(SCN)$_4$ (a) prior to and (b) after reconstruction. **q** denotes the nesting vector. (c) Lead wire configuration for magnetothermopower and Nernst effect measurements.

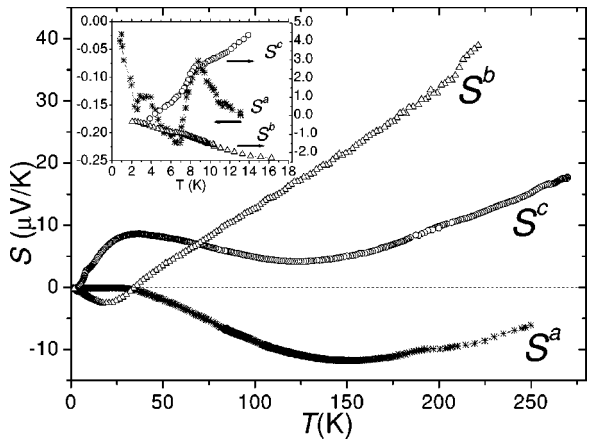

FIG. 2. Temperature dependence of the zero-field thermopower of α-(BEDT-TTF)$_2$KHg(SCN)$_4$ when the temperature gradient is applied along the *a* axis (S^a,*), the *c* axis (S^c,○), and the *b* axis (S^b,△). The inset shows the low-temperature behavior near the transition temperature T_p.

viously reported. In addition, we extend these measurements below T_p, where the thermopower reveals details of the transition into the density-wave state. *Second*, we observe, in the oscillatory magneto-thermopower (METP), quantum oscillations associated with the main closed Fermi surface orbit frequency, and also oscillations associated with the Fermi-surface reconstruction and anomalous second harmonic signals which result from the density-wave ground state. We believe that this is the first detailed study of quantum oscillations in a quasi-two dimensional organic conductor by thermopower methods. *Third*, the background (nonoscillatory) METP is sensitive to changes in the density-wave ground state with magnetic field. This includes the signatures for three changes in the Fermi surface topology, one near 3.75 T, a second above 10 T, and a third above 22.5 T. The first two are associated with magnetic breakdown effects, and the latter is the first-order phase transition to the high-field state. The temperature-magnetic field phase diagram, based on the METP results, is presented. *Finally*, in the high-field state, we describe the phase relationship between the Nernst signal and the METP signal, which is consistent with theoretical predictions.

II. BACKGROUND

The magnetic-field dependence of the thermopower in metals was previously treated theoretically. In the limit of $\omega_c\tau \gg 1$ (where ω_c is the cyclotron frequency and τ is the scattering time), asymptotic magnetotranport properties (electrical conductivity,[15] thermal conductivity[16] and thermopower[17]) are highly dependent on the Fermi-surface topology and carrier compensation, while they depend weakly on the scattering time and the energy dispersion relations. It was therefore compelling to consider the case of the magnetothermopower in α-(BEDT-TTF)$_2$KHg(SCN)$_4$, since changes in the Fermi-surface topology with increasing magnetic field should be apparent. To our knowledge, no thermopower measurements were previously carried out on the α-(BEDT-TTF)$_2$KHg(SCN)$_4$ material in very high magnetic fields.

Due to the complex nature of thermopower signals in anisotropic materials, it is useful to briefly consider previous studies in organic materials, including those at high magnetic fields where field-induced phase transitions occur. For consistency in the anisotropic thermopower parameters reported below, we use the following notation: the measured values can be written as S_{ij}^{α}, where $i,j=x,y$ or z, signifying that the heat current is applied along a geometrical direction *j* and the thermal emf is measured along a direction *i*, and α is one of the crystallographic axes along which the heat current is applied. For zero magnetic field, S_{ij}^{α} can be written in the reduced form such as S_{xx}^{α}, or simply S^{α}.

Mori *et al.*[18] performed the first in-plane measurements on α-(BEDT-TTF)$_2$KHg(SCN)$_4$, where the temperature dependence of S^a and S^c were found to be consistent with the topology of the holelike and the electronlike Fermi surfaces (see Fig. 1). Here, in general, the thermopower is positive when the thermal gradient is parallel to the open Fermi surface sheets (where holes from the cylindrical Fermi surface dominate the signal), and negative when the thermal gradient is perpendicular to the open sheets (where the electrons from the open sheets are the main contribution). Our results, shown in Fig. 2 (and to be discussed below), are in reasonable agreement with these measurements. This assignment is supported by a simulation of the thermopower, based on Boltzmann transport theory, with the bandwidth parameters as input.[18,19]

Another experiment involving in-plane thermopower has been performed on the 11.6-K organic superconductor[20] κ $-$(BEDT-TTF)$_2$Cu[N(CN)$_2$]Br (also see Gartner *et al.*[21] and Buravov *et al.*[22]). This system also has open and closed Fermi surfaces, and again, the sign of the thermopower in the normal state above T_c follows a general rule that it is positive when the thermal gradient is parallel to the electron sheets, and negative when perpendicular. Below T_c, the ther-

mopower vanished, as expected for a superconductor in zero magnetic field. In the Br-Cl alloy systems, i.e., $\kappa-(\mathrm{BEDT\text{-}TTF})_2\mathrm{Cu}[\mathrm{N(CN)_2}]\ \mathrm{Cl}_{1-x}\mathrm{Br}_x$, the thermopower takes on a more complex character.[23–25] In the nonsuperconducting $\kappa-(\mathrm{BEDT\text{-}TTF})_2\mathrm{Cu}[\mathrm{N(CN)_2}]\mathrm{Cl}$ material, the thermopower shows a $1/T$ dependence below the metal-insulator transition temperature, followed by a sharp decrease, and finally, a temperature-independent (zero) thermopower. This behavior was attributed to a weak ferromagnetic transition due to the complex electronic structure (i.e., the coexistence of 1D and 2D Fermi surfaces) of the compound.

There have been several studies of quasi-one dimensional (1D) systems based on the TCNQ charge transfer salts[26,27] and also the perylene based compounds.[28] Here, depending on the species of cations and the temperature range, the thermopower shows a linear temperature dependence, a $1/T$ behavior, or temperature independence. The different temperature dependences are described as follows. The linear decrease of thermopower has been treated with a simple, single carrier in a 1D tight-binding band model, where the temperature behavior followed a linear T dependence: $S=2\pi^2k_B^2T/3eW\cos(\pi/2\rho)/\sin^2(\pi/2\rho)$. Here W is the bandwidth and ρ is the number of carriers per site. Below the metal-to-insulator transition, the low-temperature behavior follows the $1/T$ form $S=-(k_B/e)[(c-1)/(c+1)E_g/2k_BT+3/4\ \ln(m_e/m_h)]$ where E_g is the gap and c is the ratio of the electron to hole mobilities. Finally, the temperature independent thermopower, typically with a magnitude of $\sim\pm60\ \mu$V/K, has been attributed to the spin configuration entropy $[\pm k_B/e\ (\ln 2)]$ in the strong Coulomb potential limit ($U\gg t$) in a quarter-filled band.

In the presence of an applied magnetic field, the transverse thermopower (the Nernst effect) may be measured in addition to the normal longitudinal thermopower (the Seebeck effect). Logvenov *et al.*[29] investigated the superconducting states of two $\kappa-(\mathrm{BEDT\text{-}TTF})_2X$ materials ($X=\mathrm{Cu(NCS)_2}$, $\mathrm{Cu}[\mathrm{N(CN)_2}]\mathrm{Br}$) up to 3 T. The results were interpreted in terms of flux motion and the Magnus force (in the case of the Nernst effect). The authors found considerable anisotropy, which was attributed to the difference in the electron and hole Fermi surface sections.

The quasi-one-dimensional Bechgaard salts, which exhibit a spin-density-wave (SDW) formation, have been investigated by TEP and MTEP in some detail. The SDW transition in $(\mathrm{TMTSF})_2\mathrm{AsF_6}$ at ambient pressure ($T_{SDW}=12$ K) has been investigated[30] up to 11.3 T. Hysteretic temperature effects in the thermopower were observed as a function of field direction below T_{SDW}, and the authors speculated about pinning, structural changes, and subphases associated with the SDW ground state to describe the data. For systems with magnetic-field-induced spin-density-wave (FISDW) states, two thermopower studies to 30 T have done on the quasi-one-dimensional organic conductor series $(\mathrm{TMTSF})_2\mathrm{ClO_4}$ (Ref. 31) and $(\mathrm{TMTSF})_2\mathrm{PF_6}$ under pressure.[32] In these materials a FISDW transition occurs from a quasi-1D metallic state to a sequence of SDW states. Both the MTEP and Nernst signals, which bear some relation to the corresponding transport measurements (i.e., longitudinal resistivity ρ_{xx} and the Hall effect ρ_{xy}, respectively), are sensitive to these transitions. As the final FISDW subphase is entered at constant field with lower temperatures, the thermopower first rises with an activated (gaplike) behavior, followed by a decrease at lower temperatures deeper in the SDW phase. The behavior is interpreted in terms of collective modes within the SDW phases. Notably, quantum oscillations (the so-called ''rapid oscillations'' which are periodic in inverse field) are observed in the thermopower for both materials. These experiments show the usefulness of thermopower measurements to probe ground states that are induced at high magnetic fields.

In this paper, we report thermopower measurement results carried out under high magnetic field and at low temperatures in α-$(\mathrm{BEDT\text{-}TTF})_2\mathrm{KHg(SCN)_4}$. The heat current was applied along all three crystallographic axes, and the longitudinal (Seebeck coefficient) and transverse (Nernst effect) thermopowers were measured.

III. EXPERIMENT

α-$(\mathrm{BEDT\text{-}TTF})_2\mathrm{KHg(SCN)_4}$ single-crystal samples were synthesized by conventional electrochemical crystallization techniques. The orientation of crystallographic axes were determined from polarized IR reflection measurements at room temperature. Three different samples from a single batch were used for each three different experimental conditions (heat current parallel to the *a* axis, the *c* axis, or the *b* axis). The magnetic field was always applied along the least conducting axis (*b* axis). When the heat current was applied in the most conducting plane (*ac* plane), the off-diagonal term of the thermopower tensor (S_{yx}) was measured simultaneously. The polarity of the magnetic field was switched for the measurement of S_{yx} to remove spurious components due to the misalignment of the voltage leads. (The alignment of voltage leads for S_{xx} measurements was also checked in this manner.) Thermopower measurements were carried out by applying sinusoidal heat currents along a specific crystallographic axis of the single crystal, and measuring the thermal emf in the same direction, and at 90° for S_{yx} [see Fig. 1(c)]. The sample was mounted between two quartz blocks, which were heated by sinusoidal heating currents (with an oscillation frequency $f_0=66$ mHz) with a $\pi/2$ phase difference. The corresponding temperature gradient (ΔT) and the thermal emf with $2f_0$ oscillation frequency were measured. The magnetothermopower of Au lead wires was *in situ* calibrated by $\mathrm{YBa_2Cu_3O_{7+\delta}}$ superconductor. ∇T, which was found to be nearly field independent, was set prior to each magnetic field sweep. The procedures of the magnetothermopower measurement method used in this work are detailed elsewhere.[33]

IV. RESULTS AND DISCUSSION

A. Zero-field thermopower

The temperature dependence of the zero-field thermopower for α-$(\mathrm{BEDT\text{-}TTF})_2\mathrm{KHg(SCN)_4}$, along each of the principal axes, is shown in Fig. 2, where the inset shows the low-temperature region near $T_p=8$ K. The in-plane results are in general agreement with previous measurements

by Mori *et al.*,[18] and also similar to another member of this compound $\alpha-(\text{BEDT-TTF})_2\text{TlHg(SCN)}_4$ reported by Yefanov *et al.*[34]

The negative (positive) sign of thermopower along the $a(c)$ axis indicates that the Fermi surface is electron like (hole like) along the $a(c)$ axis, which corresponds to the Fermi surface as shown in Fig. 1: here, for a thermal gradient along the *c*-axis direction, the hole pockets should contribute, whereas for the *a*-axis direction the electron like open sheets should contribute as well. We note however, that the temperature dependence of the thermopower shown in Fig. 2 is nonmonotonic. There is a minimum in S^c and S^a in the range of temperature between 120 and 150 K.

The interplane thermopower (S^b), perpendicular to the conducting planes, shows a monotonic (nearly linear) decrease down to 35 K, where it changes sign. For comparison, the interplane thermopower for α-$(\text{BEDT-TTF})_2\text{TlHg}(X\text{CN})_4$ ($X=$S or Se) also has been reported,[34,35] where S^b also shows a linear temperature dependence, but the overall magnitude is substantially less, and there is no low temperature feature observable. The origin of the differences in S^b between the K and Tl (S or Se) salts is uncertain without further study. We note that the linear T dependence for inter plane thermopower is commonly observed for both organic conductors and high-T_c superconductors,[36] which is distinctly different in form from that of the in-plane thermopower.

When the heat current is applied perpendicular to the most conducting planes, the 2D band model will not be appropriate without considering the energy dispersion between conducting planes. Furthermore, a straightforward application of the $S \approx T/W$ relationship produces unrealistic values of the *b*-axis bandwidth of order 250 meV from our results (and 50 meV from the data of Yefanov *et al.*[34]), which is known from fermiology studies to be at least 100 times (or 20 times) smaller. For $YBa_2Cu_3O_{7+\delta}$ superconductors, a phonon-assisted hopping mechanism was suggested to explain the linear *T*-dependent interplane thermopower. At present, however, there is no satisfactory treatment of either the magnetoresistance or the thermopower for the inter-plane transport behavior.

The deviation from the linear T dependence for the in-plane thermopower in the intermediate-temperature range has been treated[18,19] by Mori *et al.*, as mentioned in Sec. II above. For $\kappa-(\text{BEDT-TTF})_2\text{Cu}[\text{N(CN)}_2]\text{Br}$ (Ref. 20) and κ-$(\text{BEDT-TTF})_2\text{Cu(NCS)}_2$ (Ref. 19) salts, the same method (solving the Boltzmann equation on the Fermi surface) produces thermopower curves that reasonably describe the experimental results. For the α-$(\text{BEDT-TTF})_2\text{MHg(SCN)}_4$ salts, the computed thermopower is satisfactory for S^c over the entire temperature range (their S^c data increase monotonically). However, for S^a, the broad minimum feature cannot be accounted for by the model.

It was suggested by Merino and McKenzie that the peak in the temperature dependence of thermopower can be explained by the destruction of the Fermi liquid quasiparticles, resulting in a ''bad'' metal.[37] In this model, a smooth crossover from coherent Fermi-liquid excitations at low temperature to incoherent excitations at high temperature leads to a nonmonotonic temperature dependence in transport properties. The crossover temperature depends on relative magnitudes of the transfer integrals and the Coulomb interaction U. From our measurements, we assume that the crossover temperature is around 150 K, where S^a shows a broad minimum. A hump structure in the temperature dependence of resistivity also appears around 150 K for KHg (Ref. 38) and TlHg (Ref. 39) salts. Within this model, Eq. (1) will be applicable only below this temperature, and the high-temperature behavior should be treated more carefully.

The peak in S^c at low temperature can be explained by either model as long as the temperature range is well below the crossover temperature. This peak behavior was also observed in most thermopower measurements for α-$(\text{BEDT-TTF})_2\text{MHg(SCN)}_4$ salts, though there is a distribution of magnitudes and peak temperatures among the samples. The peak in thermopower may arise from the energy-dependent scattering term of Eq. (1), or from the phonon drag effect. The thermopower associated with phonon drag results from the electron-phonon coupling. The temperature dependence changes from a T^3 to a T^{-1} behavior[14] with increasing temperature. In particular, peak structures at low temperature (typically between $\theta_D/10$ and $\theta_D/5$, where θ_D is the Debye temperature) are usually attributed to the phonon drag effect, whose temperature dependence in noble metals is quite similar to that of S^c. Thermopower measurements on the other members of this compound [α-$(\text{BEDT-TTF})_2M\text{Hg(SCN)}_4$, where $M=$Tl, Rb, NH_4] also showed peak structures at lower temperatures (15–20 K), which were attributed to the phonon drag effect.[40] Of note is the superconductivity of the NH_4 salt, where there is an enhancement of density of states and effective mass ($m^* \approx 2.1m_0$) for [κ-$(\text{BEDT-TTF})_2\text{NH}_4\text{Hg(SCN)}_4$ over that of nonsuperconducting α-$(\text{BEDT-TTF})_2\text{KHg(SCN)}_4$ ($m^* \approx 1.5m_0$)], as pointed out by Mori *et al.*[18] However, the origin of enhancement of m^*, which may be due to electron-electron interaction and/or electron-phonon interaction, is not yet clear.

The temperature dependence of the thermopower in the vicinity of the density wave transition has been reported for the κ-$(\text{BEDT-TTF})_2\text{TlHg(SCN)}_4$ salt.[34,39] It was observed that the thermopower dropped rapidly to zero below the density-wave transition temperature T_p. The authors attributed this behavior to the collective motion of a sliding SDW below T_p. In our measurements, however, a jump rather than a drop of thermopower is observed around T_p, as shown in the inset of Fig. 2. The difference may be due to the fact that the density wave is more highly pinned in our samples. Without the sliding of density waves, the effect of opening of a gap for the open sheets would dominate the transport properties.

In electrical transport measurements, the rise in resistance near T_p may be attributed to the vanishing of conductivity contributed by carriers from the open-Fermi surface sheets (σ_{1D}), in parallel with the remaining finite conductivity of closed hole pockets (σ_{2D}).[41] In addition, for thermopower measurements, metallic carriers give a linear T dependence, while activation over a band gap gives a $1/T$ dependence. Therefore, for one type of carrier (from either open sheets or

closed pockets exclusively), the S^a will diverge below T_p. Experimentally, there is always the possibility of random diffusion of heat along the sample due to a misalignment between the heat current and the crystal axes, and, also, the total thermopower may involve a mixing of contributions from several bands (especially below T_p where the Fermi surface is reconstructed). Nevertheless, we believe that dominant behavior of thermopower in the present case reflects the influence of the heat currents with respect to the topology and orientation of the specific orbits.

When two types of carriers are involved, the total thermopower can be written as[13]

$$S_{tot}=\frac{\sigma_{1D}S_{1D}+\sigma_{2D}S_{2D}}{\sigma_{1D}+\sigma_{2D}}. \tag{2}$$

Above T_p, carriers from both Fermi surfaces have a metallic conductivity and thermopower; hence the total thermopower shows a linear temperature dependence. However, below T_p, a band gap opens for the 1D band, σ_{1D}, goes to zero exponentially as the temperature decreases, and S_{1D} diverges as $1/T$. However, below this temperature, a modified closed orbit band remains, which still gives a metallic thermopower contribution. Consequently, just below the transition temperature, there will be a jump in the thermopower ΔS from the divergence of S_{1D}, but this contribution quickly disappears as σ_{1D} goes to zero.

It is interesting to compare the temperature dependence of resistivity and thermopower of the quasi-1D Bechgaard salts with the KHg salt, since, for the Bechgaard salts, the entire Fermi surface is involved in the spin-density-wave formation. Since there is only one band to nest, both the resistivity and the thermopower in the Bechgaard salts show an activated behavior below the transition temperature. In addition, in the vicinity of the SDW transition, an anomalous feature arises in the thermopower.[30,42,43] The anomaly is consistent with a theoretical treatment of the thermopower at the SDW transition. Here a strong singularity is predicted in the temperature derivative of the thermopower at the anitiferromagnetic ordering temperature.[44] In our data, we do not observe any singularity at T_p, nor do we see activated behavior at lower temperatures. Since in α-(BEDT-TTF)$_2$KHg(SCN)$_4$ not all the Fermi surface is nested, we would not expect activated behavior below T_p. Likewise, we would not expect a strong singularity at T_p, particularly if the transition is not to a conventional SDW state.

We may further compare the magnitude of jump of the thermopower (ΔS) with that of the electronic heat capacity (ΔC_{el}). Since the thermopower measures the heat carried by a carrier, divided by the carrier charge and temperature, ΔS is equal to $\Delta C_{el}/e$. Adding both contributions from S^a and S^c, ΔS is about 1 μV/K, which corresponds to $1/6.24\times10^{-24}$ J/K carrier. Reports for ΔC_{el} are in the range 0.1 J/mol K (Ref. 45) to 0.25 J/mol K,[46] both of which are in fair agreement with ΔS computed from our data. A corresponding change in S^b at T_p is unclear, if it exists at all (in Fig. 2). This indicates that the phase transition around $T_p=8$ K occurs predominantly within the in-plane electronic structure.

B. Magnetothermopower

In Fig. 3, we present the magnetic-field dependence of the TEP (i.e., MTEP) for all three crystallographic directions at different, fixed temperatures. To show the field dependence more clearly, some traces are offset from zero as indicated by the dashed lines. The MTEP signal contains two components, the background MTEP which is sensitive to the Fermi surface topology, and the oscillatory MTEP which is a manifestation of the Landau quantization of the closed orbit Fermi surface. To separate the two signals, in Fig. 4 we show the background MTEP data, where the oscillatory MTEP has been removed by filtering out the total MTEP signal. Finally, the Nernst effect at different temperatures is shown in Fig. 5. In all cases the magnetic field is applied along the b axis, perpendicular to the $a-c$ conducting plane.

A similarity between the magnetic-field dependence of the thermopower and the resistance can be expected from the Boltzmann transport equations. Indeed, we find that the general field dependence of the MTEP is similar in some respects to that of the magnetoresistance.[4] (1) Below T_p, the in-plane MTEP shows a broad peak at $B(=B_A)\sim10$ T. (2) Above the ''kink field'' B_k at 22.5 T, the field dependence is weak. (3) Quantum oscillations are observed in the MTEP signal associated with the de Haas–van Alphen (dHvA) and Shubnikov–de Haas (SdH) effects [i.e., from Eq. (7) below, both thermodynamic and transport properties are involved in the thermopower]. The oscillation amplitudes are largest for S^c_{xx}, and the oscillations are also observed in S^b_{zz}. (4) The MTEP also shows hysteresis for up and down field sweeps. Beyond the general comparison between resistivity and MTEP, unique field-dependent features are observed in the MTEP and Nernst signals:

(1) For S^a_{xx} and S^c_{xx}, the MTEP exhibits a minimum at $B=B_{min}$ after which it rapidly increases up to maximum at $B=B_A$. B_{min} is also temperature dependent, and decreases with increasing temperature.

(2) For the a-axis behavior, the Nernst signal S^a_{yx} shows a similar field dependence to the MTEP signal S^a_{xx} in general, but S^a_{yx} is asymptotic to zero above B_k for all temperatures measured. In contrast, S^a_{xx} is asymptotic to non-zero, temperature dependent values above B_k.

(3) For the c-axis behavior, S^c_{yx} shows a linear field dependence at higher field, which is distinct from the other thermopower coefficients.

(4) For the b axis, S^b_{zz} exhibits some aspects of S^a_{xx} and S^c_{xx} mentioned above, which may involve some mixing of the in-plane components.

Figure 6 shows the temperature dependence of magnetothermopower for a fixed magnetic field. As the magnetic field is increased, the transition temperature T_p, represented as a jump or shoulder in the data, shifts to lower temperature. (For S^b_{zz} and S^c_{xx} at $B=27$ T, however, T_p could not be resolved.) The temperature-field phase diagram, based exclusively on the field and temperature-dependent thermopower data [B_{min}, B_A, B_k, and $T_p(B)$], is shown in Fig. 7. The phase diagram is very similar (with the exception of the new B_{min} line) to previous determinations by transport,[47–50] NMR,[51,52] magnetization,[10,53] and specific heat.[54]

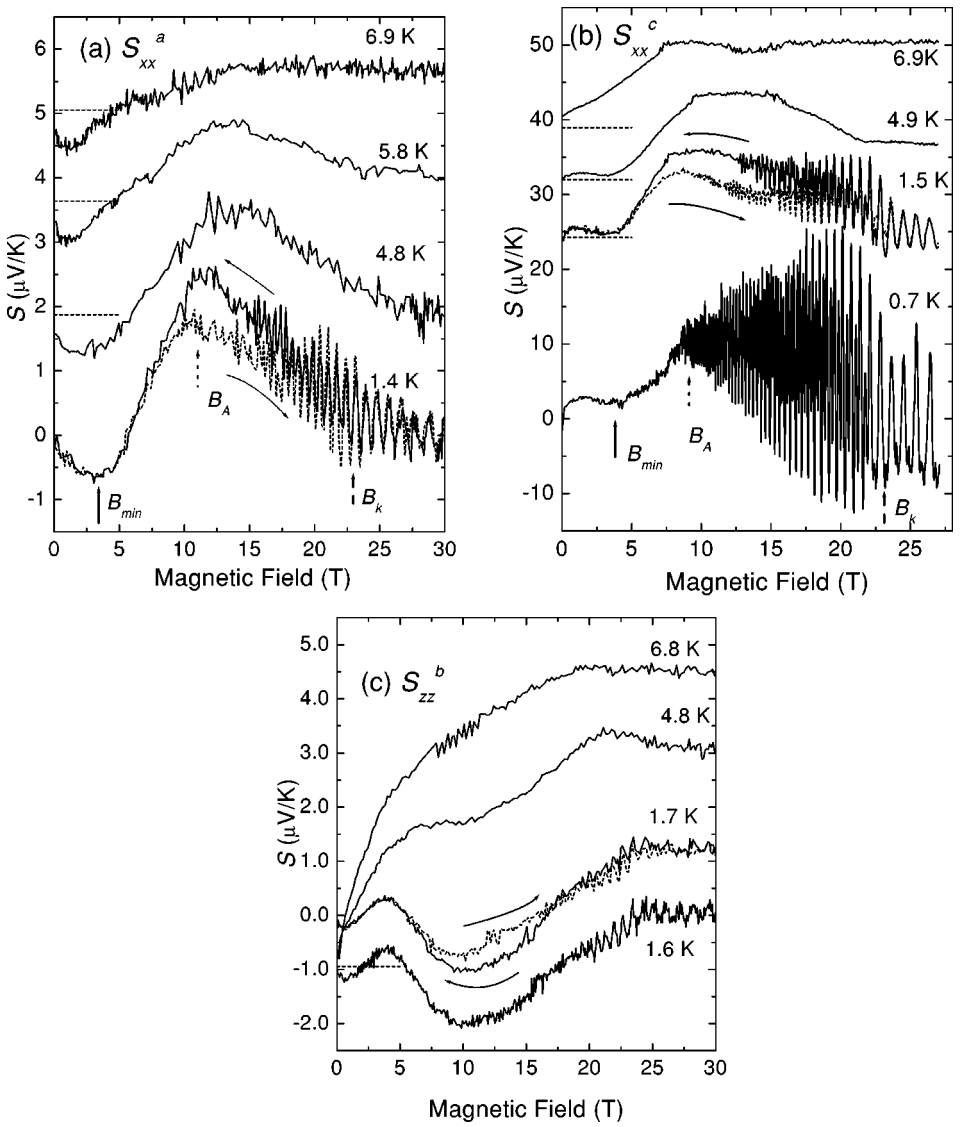

FIG. 3. Magnetothermopower of (a) S^a, (b) S^c, and (c) S^b for field sweeps (decreasing). Field sweep data for both directions are shown for $T \sim 1.5$ K. The arrows indicate characteristic fields as defined in the text. Shifted zeros for some data sets are indicated by dashed lines. For unshifted data, see Fig. 4.

1. Theoretical aspects of high field thermopower measurements

To interpret the origin of the field dependence of the MTEP, it is useful to examine the magnetic-field dependence of the thermopower for an anisotropic system. When the thermopower is measured in a magnetic field, the tensor elements of thermopower should be considered, since both the temperature gradient and the magnetic field are vectorial. For our experimental conditions (zero electric current and zero transverse heat current), the kinetic equations for thermopower and heat currents can be written as

$$E_i = \alpha_{ij} \nabla T_j, \quad (J_q)_i = -K_{ij} \nabla T_j, \tag{3}$$

where E is the electric field produced by the thermal emf, α is the thermopower tensor under a magnetic field, J_q is the heat current, and K is the thermal conductivity tensor. We have two different experimental situations.

(a) H parallel to the z axis, parallel to J_q, and parallel to ∇T_z (S_{zz}^b in this paper). In this case, no Lorentz force is applied so that $\nabla T_x = \nabla T_y = 0$, and the above equations have simple scalar forms

$$E_z = \alpha_{zz} \nabla T_z, \quad (J_q)_z = -K_{zz} \nabla T_z. \tag{4}$$

The measured value S_{zz}^b is obtained from $E_z / \nabla T_z$.

(b) H parallel to the z axis and perpendicular to J_q (S_{xx}^a, S_{yx}^a, S_{xx}^c and S_{yx}^c in this paper). In this case, ∇T is not parallel to J_q, and has a nonzero y component given by $\nabla T_y = -\nabla T_x K_{yx} / K_{yy}$. If we rewrite Eq. (3) for this case,

$$\begin{pmatrix} E_x \\ E_y \end{pmatrix} = \begin{pmatrix} \alpha_{xx} & \alpha_{xy} \\ \alpha_{yx} & \alpha_{yy} \end{pmatrix} \begin{pmatrix} \nabla T_x \\ -\nabla T_x K_{yx} / K_{yy} \end{pmatrix}. \tag{5}$$

In terms of measured values, Eq. (5) can be expressed as

$$S_{xx} = \frac{E_x}{\nabla T_x} = \alpha_{xx} - \alpha_{xy} \frac{K_{yx}}{K_{yy}},$$

$$S_{yx} = \frac{E_y}{\nabla T_x} = \alpha_{yx} - \alpha_{yy} \frac{K_{yx}}{K_{yy}}. \tag{6}$$

The asymptotic behavior of thermoelectric tensor α_{ij} (Ref. 17) and thermal conductivity tensor K_{ij} (Ref. 16) were cal-

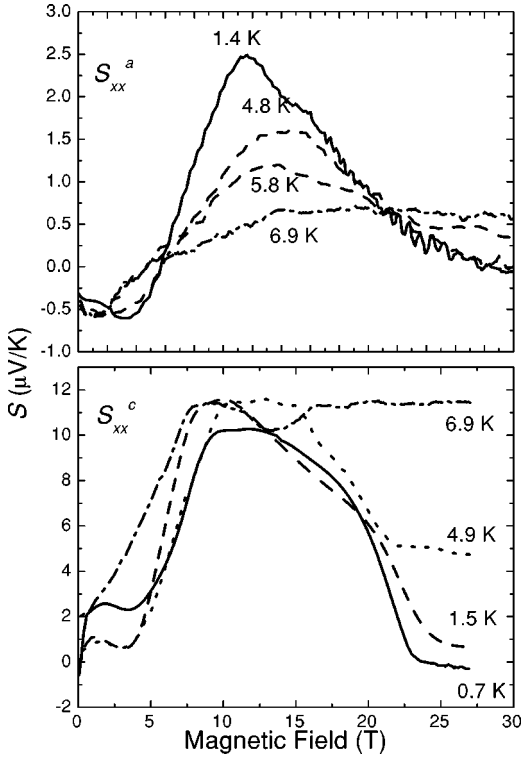

FIG. 4. Background magnetothermopower of S^a and S^b obtained from Fig. 3 by filtering out the quantum oscillation component.

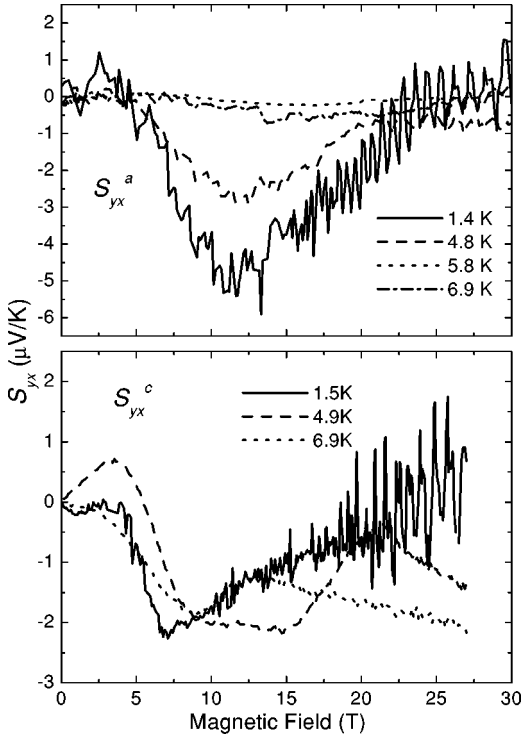

FIG. 5. Nernst effect of α-(BEDT-TTF)$_2$KHg(SCN)$_4$ when the heat current is applied along the a axis (S_{yx}^a) and the c axis (S_{yx}^c).

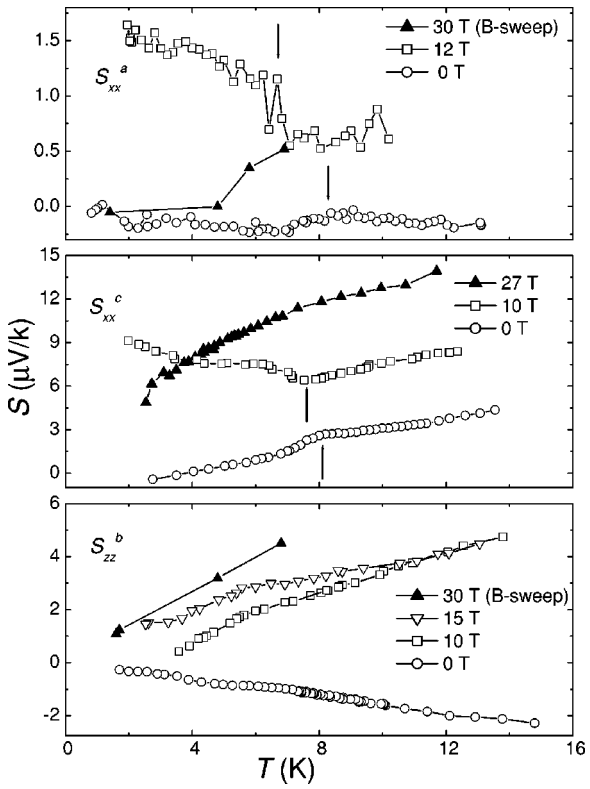

FIG. 6. Temperature dependence of magnetothermopower of α-(BEDT-TTF)$_2$KHg(SCN)$_4$, measured under a fixed magnetic field. Arrows indicate the transition temperature T_p. Due to complications associated with the changes in the quantum oscillation amplitudes, the 30-T background data from Fig. 4 has been used for S^a and S^b.

culated at low temperature and high magnetic field. They show different behaviors for the three different cases, i.e., (a) closed and compensated orbits, (b) closed and uncompensated orbits, and (c) open orbits along the x direction. For each case, the asymptotic behaviors of S_{ij} can be calculated

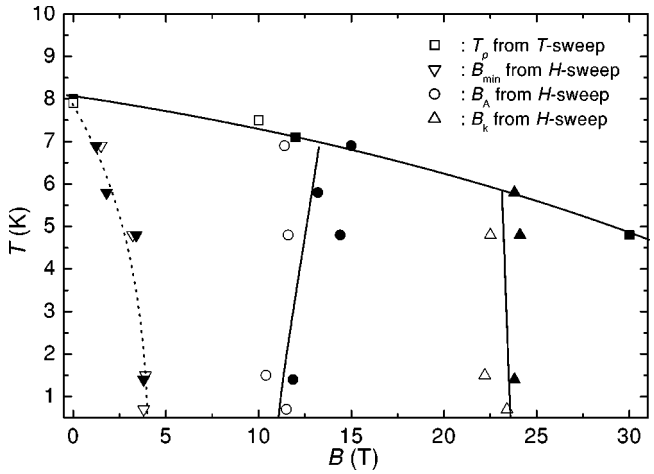

FIG. 7. T-B Phase diagrams of α-(BEDT-TTF)$_2$KHg(SCN)$_4$ drawn from S_{xx}^a and S_{xx}^c. T_p is obtained from the temperature sweep and B_{min}, B_A, and B_k are obtained from the field sweep. Open symbols are from S_{xx}^a, and solid symbols from S_{xx}^c.

TABLE I. High-field power-law behavior (H^{γ} where $\gamma=1,0,$ and -1) of the magnetothermopower for different types of orbits.

	Closed compensated	Closed uncompensated	Open along the x direction
K_{yx}/K_{yy}	H^0	H^1	H^{-1}
α_{xx},α_{yy}	H^1	H^0	H^0
α_{xy}	H^1	H^{-1}	H^1
α_{yx}	H^1	H^{-1}	H^{-1}
α_{zz}	H^0	H^0	H^{-1}
S_{xx}	H^1	H^0	H^0
S_{yx}	H^1	H^1	H^{-1}
S_{zz}	H^0	H^0	H^0

and the results are summarized in Table I. The saturation values are temperature dependent for each case, and they should be determined by considering the scattering and the dispersion relations.

2. Comparison of theoretical and experimental MTEP results

We now compare the thermopower data with the theoretical field dependence described above. We focus our attention on the behavior of the S^c signal shown in Figs. 3 and 4, since it is significantly larger than the other signals, and it is predominantly holelike (i.e., positive, and closed hole pocket sensitive). As a guide we may use the detailed work by Uji *et al.*[55] on the fermiology study of the quantum oscillations, due to closed orbits in the magnetic breakdown network, which were proposed to describe the Fermi-surface topology for $T<T_p$ (also see the discussion of reconstructed Fermi surface by Harrison *et al.*[56] below). In this model, it is assumed that only small closed orbit pockets exist in the reconstructed Fermi surface below T_p near a zero magnetic field. As the magnetic field is increased, larger and larger Fermi surface sections become involved in the SdH oscillations as magnetic breakdown becomes more probable. These effects appear experimentally in the SdH measurements: in Figs. 8 and 9 of Ref. 55, the onset of the SdH oscillations associated with the various magnetic breakdown orbits (α, ϕ, etc.) occurs above 3.5 T. At higher fields, above 7 T, the β orbit associated with the Brillouin zone appears. Finally, above the kink field, the original Fermi surface topology (as in Fig. 1) re-emerges.

In light of the above, our first point of comparison is the behavior of B_{min}. For S^c, and indeed in all MTEP directions, there is a distinct change in the signal above B_{min} from a relatively flat response to a pronounced increase in slope (approximately linear) with field. This behavior is entirely consistent with the theoretical model above for a set of closed, compensated orbits.

At higher fields, above B_A, the compensated closed orbit behavior of S^c changes dramatically, and this indicates that the magnetic breakdown network of closed orbits is undergoing a modification with increasing field. By comparison with the theory above, we may speculate that this is the onset of uncompensated closed orbit behavior, which exhibits less (eventually no) field dependence.

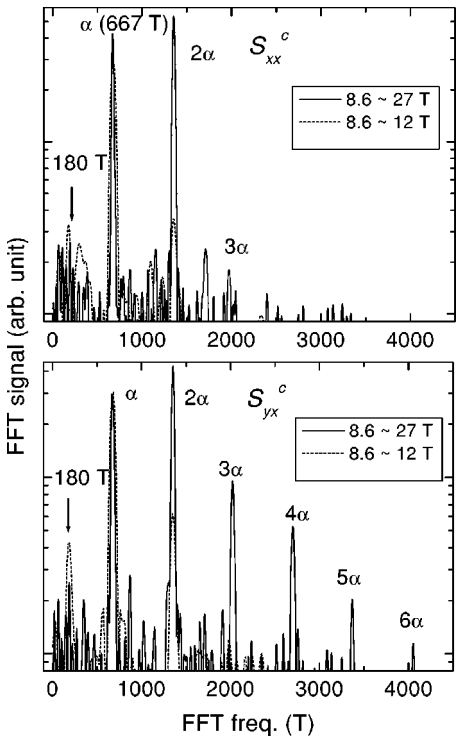

FIG. 8. FFT spectrum for S^c_{xx} and S^c_{yx} at $T=0.7$ and 1.5 K for 8.6 T $\leqslant B \leqslant$ 12 T and 8.6 T $\leqslant B \leqslant$ 27 T. The fundamental frequency of the closed hole orbit (α orbit) and its higher harmonics are clearly shown. The peak at 180 T is the ϕ orbit, as discussed in Ref. 55.

Finally, above the kink field, the original, uncompensated closed orbit FS is realized, and the field dependence disappears, as is evident from the S^c data. Above B_k, we may compare the temperature dependence of S^c with those at zero field above T_p (see Fig. 6). Except for the field-dependent offsets, the thermopower above $T_p(B)$ for the three directions is similar, save for the case of S^b which is anomalous, even in the absence of field.

Beyond this simple comparison of the most dominant MTEP signal with previous SdH studies and theoretical expectations, the assignment the mechanisms responsible for the magnetic field dependence of S^a and S^b are more speculative. This is due to the apparent mixing of terms in the experimental data, and to sort them out is beyond the scope of the present work. However, the Nernst data show significant differences for the a and c axes (S^a_{yx} and S^c_{yx}). This is most apparent above B_k, where the original Fermi surface is expected to be recovered. Here S^a_{yx} is seen to be asymptotic to zero (i.e., H^{-1} dependence), while S^c_{yx} clearly assumes a linear (i.e., H^1) dependence.

Of note is the Fermi-surface reconstruction proposed by Harrison *et al.*, who fitted the tight-binding band parameters using the SdH, dHvA, and angle-dependent magnetoresistance oscillation data.[56] The resulting Fermi surface is different from that derived from SdH data by Uji *et al.*,[55] but the general features of the MTEP are consistent with either model. However, one difference between two models is the existence of open sheets on the Fermi surface after recon-

struction. According to Harrison *et al.*, the nesting of the original open sheets is imperfect, which results in a new set of quasi-1D sheets with different orientations. If we compare our experimental results (vanishing S_{yx}^{a} and increasing S_{yx}^{c}) with the asymptotic behavior of S_{yx} in Table I, the existence of open sheets seems to be more likely.

3. MTEP and Landau quantization

Equation (1) can be rewritten in the alternative form[13]

$$S=\frac{\pi^2 k_B^2}{3e}T\left(\frac{d\ln n(\epsilon)}{d\epsilon}+\frac{d\ln v^2(\epsilon)}{d\epsilon}+\frac{d\ln \tau(\epsilon)}{d\epsilon}\right)\Bigg|_{\epsilon=\epsilon_F}, \tag{7}$$

where $n(\epsilon)$ is the density of the states, $v(\epsilon)$ is an average charge velocity, and $\tau(\epsilon)$ is the carrier scattering relaxation time. From this equation, it is clear that for a quasi-two dimensional Fermi surface, the magnetic- field dependence of the Landau-level spectrum[57] will produce quantum oscillations in the thermopower, which will originate from both thermodynamic and electron transport factors. The latter was treated by Zil'berman[58] and Long *et al.*,[59] where scattering between states of the Landau-level closest to the Fermi surface and states of other occupied were considered. In our results we find a clear indication of the Landau-level spectrum in the MTEP and Nernst data, the periodicity of which is in good agreement with previous SdH and dHvA measurements.[60] In particular, the oscillation frequency obtained from the fast Fourier transform (FFT) analysis of S_{xx}^{c} and S_{yx}^{c} at 0.7 K (see Fig. 8) is about 667 T, which agrees with results obtained from other measurements.[55] This comparison also includes the observation of higher harmonics of the fundamental α orbit, and even the ϕ orbit (180 T) which is expected to be a manifestation of the magnetic breakdown topology below B_k. (See, for instance Uji *et al.*[55]) There is another explanation for the origin of the 180-T oscillation in terms of a quantum interference effect.[56] This is based on the observation that the 180-T frequency is only observed in resistivity (SdH), and not in magnetization (dHvA). In the present case, for MTEP measurements, we cannot rule out such possibilities since thermopower probes both transport and thermodynamic properties.

An important feature of our results, most evident above B_k, is a phase difference between the METP and Nernst quantum oscillations. This is shown in Fig. 9 for two different cases, the *a*, and *c* axes. Indeed, Zil'berman's model[58] (also see Ref. 59, predicted a phase difference of π between the MTEP and Nernst oscillations. We show this more explicitly for S_{xx}^{c} and S_{yx}^{c} at $T=0.7$ K in Fig. 10 , with the angle (θ) defined as the ratio of the electric fields due to transverse and longitudinal thermopower [$\theta=\arctan(S_{yx}/S_{xx})=\arctan(E_y/E_x)$]. The phase difference is π, which supports Zil'berman's model.[56]

Zil'berman's model also predicted similar field and temperature dependences of the oscillation amplitude with that of the Lifschitz-Kosevich (LK) formula for de Haas–van Alphen oscillations. The amplitude of thermopower oscillation increases when $B_A<B<B_k$, but it is almost field independent above B_k. We note that in this range of temperature, the quantum oscillation amplitude is complicated due to the anomalous high field state, where the dHvA and SdH oscillations behave in a significantly different manner, and a comparison based on standard LK theory is not applicable. A more systematic study of the MTEP and Nernst effects above B_k vs temperature, and also vs field orientation, will be necessary to provide a complete picture.

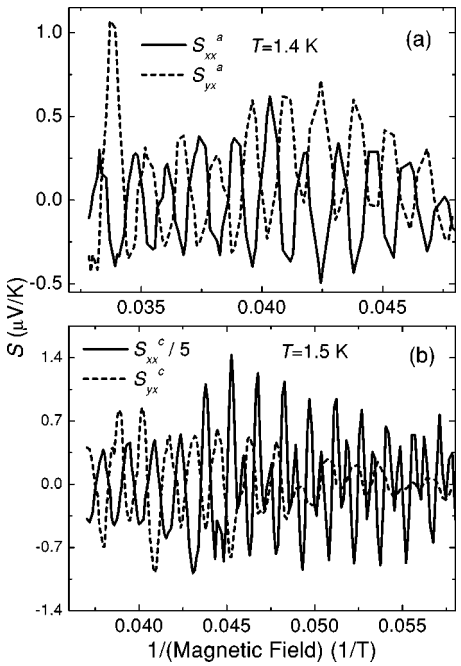

FIG. 9. Transverse and longitudinal magnetothermopower oscillation as a function of inverse magnetic field in the high-field region for (a) S^a and (b) S^c. The background magnetothermopower was subtracted and the amplitude of S_{xx}^{c} was divided by 5.

4. Thermopower above the kink field B_k

One final important question is the nature of the thermopower in the high-field state. This is in light of the specu-

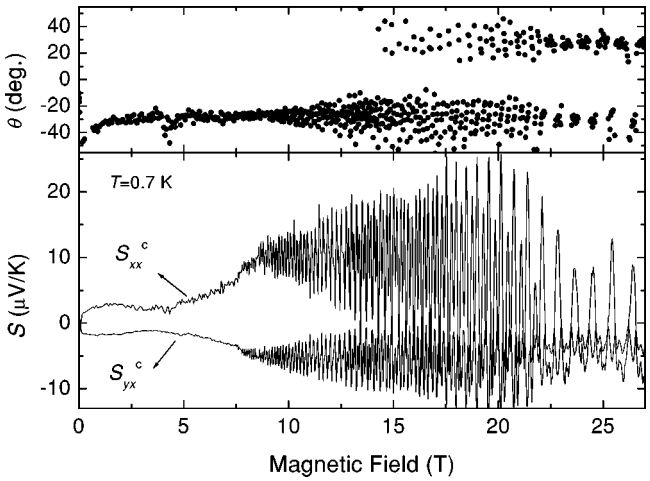

FIG. 10. Comparison of the phases of oscillations between S_{xx}^{c} and S_{yx}^{c} at $T=0.7$ K, and a plot of arctan (S_{xx}^{c}/S_{yx}^{c}) as a function of the magnetic field.

lations mentioned previously concerning a critical state (possibly superconducting) behavior associated with a CDW ground state[10,11] above the kink field B_k. Based on the simple notion that the thermopower should vanish in a superconducting state, we consider the behavior of the MTEP above the kink field B_k. Referring to the background MTEP data shown in Figs. 4 and 6, we note that the thermopower signal in the range between B_k and 30 T decreases with decreasing temperature for all three crystallographic directions. This is accompanied by a reduced amplitude of the quantum oscillations (see Fig. 3) above B_k. However, the thermopower remains finite. This is in contrast to the behavior for a superconducting ground state, where S should strictly be zero. Nevertheless, it is clear that some mechanism is driving the thermopower to lower values in the high-field state. This decrease of thermopower seems to be consistent with previous findings above B_k,[10,11] where evidence of enhanced conductivity in the magnetization and susceptibility is observed.

V. CONCLUSION

We have applied the method of magnetothermopower to investigate the low-temperature, magnetic-field-dependent phase of the anisotropic organic conductor α-(BEDT-TTF)$_2$KHg(SCN)$_4$. Our results show that the sensitivity of thermopower to anisotropic Fermi-surface topologies may be extended to the study of systems where temperature and magnetic field alter these topologies. The most significant results of the present investigation include the determination of the low temperature phase diagram of α-(BEDT-TTF)$_2$KHg(SCN)$_4$, based purely on thermopower measurements, the study of the onset of magnetic breakdown effects via the magnetothermopower, and the measurement of quantum oscillations in the magnetothermopower and Nernst effect, which are in accord with theoretical expectations.

ACKNOWLEDGMENTS

The authors would like to thank R. McKenzie and N. Harrison for important discussions. This work was carried out at the National High Magnetic Field Laboratory, which is funded by a cooperative agreement between the National Science Foundation and the State of Florida through Grant No. NSF-DMR 00-84173. J. S. B. acknowledges support from Grant No. NSF-DMR-99-71474 for this work, and E. S. C. acknowledges post-doctoral support from KOSEF.

*Present address: Physics Dept., Wake Forest University, Winston-Salem, North Carolina 27109.

[1] H. Mori, S. Tanaka, M. Oshima, G. Saito, T. Mori, Y. Maruyama, and H. Inokuchi, Bull. Chem. Soc. Jpn. **63**, 2183 (1990).
[2] M.V. Kartsovnik, A.E. Kovalev, and N.D. Kushsch, J. Phys. I **3**, 1187 (1993).
[3] M.V. Kartsovnik and V.N. Laukin, J. Phys. I **6**, 1753 (1996).
[4] T. Sasaki, A.G. Lebed, T. Fukase, and N. Toyota, Phys. Rev. B **54**, 12 969 (1996).
[5] J. Wosnitza, Current Opin. Solid State Mat. Sci. **5**, 131 (2001).
[6] T. Osada, R. Yagi, A. Kawasumi, N. Miura, M. Oshima, and G. Saito, Phys. Rev. B **41**, 5428 (1990).
[7] J.S. Qualls, L. Balicas, J.S. Brooks, N. Harrison, L.K. Montgomery, and M. Tokumoto, Phys. Rev. B **62**, 10 008 (2000).
[8] C. Proust, A. Audouard, A. Kovalev, D. Vignolles, M. Kartsovnik, L. Brossard, and N. Kushch, Phys. Rev. B **62**, 2388 (2000).
[9] A. Bjelis, D. Zanchi, and G. Montambaux, J. Phys. IV **9**, 203 (1999).
[10] N. Harrison, L. Balicas, J.S. Brooks, and M. Tokumoto, Phys. Rev. B **62**, 14 212 (2000).
[11] N. Harrison, C.H. Mielke, A.D. Christianson, J.S. Brooks, and M. Tokumoto, Phys. Rev. Lett. **86**, 1586 (2001).
[12] N.A. Fortune, M.A. Elben, S. Uji, H. Aoki, J. Yamada, S. Tanaka, S. Make, S. Nakatsuji, and H. Anzai, Synth. Met. **103**, 2078 (1999).
[13] D.K.C. Mcdonald, *Thermoelectricity*, (Wiley, New York, 1962).
[14] P.M. Chaikin, in *Organic Superconductivity*, edited by V.Z. Kresin and W.A. Little, (Plenum, New York, 1990) p. 101.
[15] I.M. Lifshitz, M.Ya. Azbel, and M.I. Kaganov, Zh. Éksp. Teor. Fiz. **31**, 63 (1955) [Sov. Phys. JETP **4**, 41 (1957)].
[16] M.Ya. Azbel, M.I. Kaganov, and I.M. Lifshitz, Zh. Éksp. Teor. Fiz. **32**, 1188 (1957) [Sov. Phys. JETP **5**, 967 (1957)].
[17] Yu.A. Bychkov, L.É. Gurevich, and G.M. Nedlin, Zh. Éksp. Teor. Fiz. **37**, 534 (1959) [Sov. Phys. JETP **37**, 377 (1960)].
[18] T. Mori, H. Inokuchi, H. Mori, S. Tanaka, M. Oshima, and G. Saito, J. Phys. Soc. Jpn. **59**, 2624 (1990).
[19] T. Mori and H. Inokuchi, J. Phys. Soc. Jpn. **57**, 3674 (1988).
[20] R.C. Yu, J.M. Williams, H.H. Wang, J.E. Thompson, A.M. Kini, K.D. Carlson, J. Ren, M.-H. Whangbo, and P.M. Chaikin, Phys. Rev. B **44**, 6932 (1991).
[21] S. Gartner, E. Gogu, L. Heinen, H.J. Keller, T. Klutz, and D. Schweitzer, Solid State Commun. **65**, 1531 (1988).
[22] L.I. Buravov, N.D. Kushch V.A. Merzhanov, M.V. Osherov, A.G. Khomenko, and E.B. Yagubskii, J. Phys. I **2**, 1257 (1992).
[23] V.A. Bondarenko, Yu.V. Sushko, V.I. Barchuk, V.S. Yefanov, V.V. Dyakin, M.A. Tanatar, N.D. Kushch, and E.B. Yagubskii, Synth. Met. **56**, 2386 (1993); V.A. Bondarenko, V.V. Dyakin, V.S. Yefanov, N.D. Kushch, and E.B. Yagubskii, *ibid.* **56**, 2391 (1993).
[24] V.A. Bondarenko, R.A. Petrosov, M.A. Tanatar, V.S. Yefanov, and N.D. Kushch, Physica C **235-240**, 2467 (1994).
[25] M.A. Tanatar, V.S. Yefanov, V.V. Dyakin, V.A. Bondarenko, N.D. Kushch, and E.B. Yagubskii, Pis'ma Zh. Éksp. Teor. Fiz. **59**, 682 (1994) [JETP Lett. **59**, 720 (1994)]; M.A. Tanatar, V.S. Yefanov, M.V. Kartsovnik, A.E. Kovalev, V.A. Bondarenko, and N.D. Kushch, Synth. Met. **70**, 941 (1995).
[26] P.M. Chaikin, R.L. Greene, S. Etemad, and E. Engler, Phys. Rev. B **13**, 1627 (1976).
[27] P.M. Chaikin, J.F. Kwak, and A.J. Epstein, Phys. Rev. Lett. **42**, 1178 (1979).
[28] K. Bender, D. Schweitzer, and H.J. Keller, J. Phys. (Paris), Colloq. **44**, 1433 (1983).
[29] G.Yu. Logvenov, M.V. Kartsovnik, H. Ito, and T. Ishiguro, Synth. Met. **86**, 2023 (1997).
[30] V.A. Bondarenko, S. Kagoshima, M. Maesato, T. Hasegawa, N. Miura, and T. Yamaguchi, Solid State Commun. **107**, 477 (1998).

[31] R.C. Yu, L.Y. Chiang, R. Upasani, and P.M. Chaikin, Phys. Rev. Lett. **65**, 2458 (1992).
[32] W. Kang, S.T. Hannahs, L.Y. Chiang, R. Upasani, and P.M. Chaikin, Phys. Rev. B **45**, 13 566 (1992).
[33] E.S. Choi, J.S. Brooks, J.S. Qualls, and Y.S. Song, Rev. Sci. Instrum. **72**, 2392 (2001); physics/0009054 (unpublished).
[34] V.S. Yefanov, M.A. Tanatar, V.A. Bondarenko, N.D. Kushch, and E.B. Yagubskii, Physica C **235-240**, 2465 (1994).
[35] L.I. Buravov, N.D. Kushch, V.N. Laukhin, A.G. Khomenko, E.B. Yagubskii, M.V. Kartsovnik, A.E. Kovalev, L.P. Rozenberg, R.P. Shibaeva, M.A. Tanatar, V.S. Yefanov, V.V. Dyakin, and V.A. Bondarenko, J. Phys. I **4**, 441 (1994).
[36] D.Y. Xing, M. Liu, and C.S. Ting, Phys. Rev. B **38**, R11 992 (1988), and references therein.
[37] J. Merino and R.H. McKenzie, Phys. Rev. B **61**, 7996 (2000).
[38] H. Ito, H. Kaneko, T. Ishiguro, H. Nishiyama, H. Ishimoto, and G. Saito, Synth. Met. **56**, 2228 (1993).
[39] M.A. Tanatar, V.S. Yefanov, V.V. Dyakin, V.A. Bondarenko, N.D. Kushch, and E.B. Yagubskii, Synth. Met. **56**, 2419 (1993).
[40] S.V. Demishev, M.V. Kondrin, V.V. Glushkov, N.E. Sluchanko, and N.A. Samarin, Zh. Éksp. Teor. Fiz. **113**, 323 (1998) [JETP **86**, 182 (1998)].
[41] J.S. Brooks, G.J. Athas, S.J. Klepper, X. Chen, C.E. Campos, S. Valfells, Y. Tanaka, T. Kinoshita, N. Kinoshita, M. Tokumoto, and H. Anzai, Physica B **201**, 449 (1994).
[42] K. Bechgaard, C.S. Jacobsen, K. Mortensen, H.J. Pedersen, and N. Thorup, Solid State Commun. **33**, 1119 (1980).
[43] K. Mortensen, Solid State Commun. **44**, 643 (1982).
[44] M. Ausloos, Solid State Commun. **21**, 373 (1977).
[45] A. Kovalev, H. Mueller, and M.V. Kartsovnik, Zh. Éksp. Teor. Fiz. **113**, 1058 (1998) [JETP **86**, 578 (1998)].
[46] P.F. Henning, J.S. Brooks, J.E. Crow, Y. Tanaka, T. Kinoshita, N. Kinoshita, M. Tokumoto, and H. Anzai, Solid State Commun. **95**, 691 (1995).
[47] N. Biskup, J.A.A.J. Perenboom, J.S. Brooks, and J.S. Qualls, Solid State Commun. **107**, 503 (1998).
[48] T. Sasaki, S. Endo, and N. Toyota, Phys. Rev. B **48**, 1928 (1993).
[49] R. Mckenzie, G.J. Athas, J.S. Brooks, R.G. Clark, A.S. Dzurak, R. Newbury, R.P. Starrett, A. Skougarevsky, M. Tokumoto, N. Kinoshita, T. Kinoshita, and Y. Tanaka, Phys. Rev. B **54**, R8289 (1996).
[50] V.N. Topnikov, S.I. Pesotskii, and V.N. Laukhin, Pis'ma Éksp. Teor. Fiz. **59**, 374 (1994) [JETP Lett. **59**, 374 (1994)].
[51] K. Miyagawa, A. Kawamoto, and K. Kanoda, Phys. Rev. B **56**, R8487 (1997).
[52] P. Kuhns, J.S. Brooks, T. Caldwell, W.G. Moulton, A.P. Reyes, N. Biskup, A.M. Kini, J.A. Schlueter, H.H. Wang, U. Geiser, and J.M. Williams, Solid State Commun. **109**, 637 (1999).
[53] M.V. Kartsovnik, W. Biberacher, E. Steep, P. Christ, K. Andres, A.G.M. Jansen, and H. Mueller, Synth. Met. **86**, 1933 (1997).
[54] A. Kovalev, H. Mueller, and M.V. Kartsovnik, Zh. Éksp. Teor. Fiz. **113**, 1058 (1998) [JETP **86**, 578 (1998)].
[55] S. Uji, T. Terashima, H. Aoki, J.S. Brooks, M. Tokumoto, N. Kinoshita, T. Kinoshita, Y. Tanaka, and H. Anzai, Phys. Rev. B **54**, 9332 (1996).
[56] N. Harrison, E. Rzepniewski, J. Singleton, P.J. Gee, M.M. Honold, P. Day, and M. Kurmoo, J. Phys.: Condens. Matter **11**, 7227 (1999).
[57] I.M. Lifshitz and A.M. Kosevich, Zh. Éksp. Teor. Fiz. **29**, 730 (1955) [Sov. Phys. JETP **2**, 636 (1957)].
[58] G.E. Zil'berman, Zh. Éksp. Teor. Fiz. **29**, 762 (1955) [Sov. Phys. JETP **2**, 650 (1956)].
[59] J.R. Long, C.G. Grenier, and J.M. Reynolds, Phys. Rev. **140**, A187 (1965).
[60] J. Wosnitza, *Fermi Surfaces of Low-Dimensional Organic Metals and Superconductors*, (Springer-Verlag, Berlin, 1996).